Sādhanā (2020)45:159
https://doi.org/10.1007/s12046-020-01402-5

Application of temporal moments to interpret solute transport with time-dependent dispersion

ABHAY GULERIA[1,*], DEEPAK SWAMI[1], NITIN JOSHI[2] and ABHIMANYU SHARMA[1]

[1]School of Engineering, Indian Institute of Technology Mandi, Kamand 175005, India
[2]Department of Civil Engineering, Indian Institute of Technology Jammu, Jammu 181221, India
e-mail: abhayguleria92@gmail.com

MS received 17 February 2019; revised 12 May 2020; accepted 21 May 2020

Abstract. Temporal moments of solute transport through porous media are calculated to analyze the time average spatial distribution of solute plume. Simulation of spatially and temporally distributed breakthrough curves (BTCs) is computationally rigorous and lacking the explanation about overall plume evolution within porous media. However, temporal moment provides an attractive and simple solution to study the plume behavior. In this study, temporal moments are presented to interpret solute plume behavior in heterogeneous porous media such as hydraulically coupled stratified porous media with different time-dependent dispersion models. Governing equations of solute transport have been solved numerically using Crank-Nicolson scheme, and further solute concentration data has been utilized to calculate moments of solute concentration using numerical integration. The effect of various parameters such as mass-transfer coefficient, pore-water velocity, time-dependent dispersion coefficients, and porosity of mobile region on the transport of solute has been studied through sensitivity analyses. Temporal moment analysis revealed that the mass recovery, mean residence time, and variance are sensitive to the estimated parameters. Numerical results suggested that the asymptotic time-dependent dispersion function with mobile–immobile model represents the plume spreading through heterogeneous porous media in a more realistic manner.

Keywords. Moment analysis of solute concentration; heterogeneous porous media; mobile–immobile model; mass-transfer coefficient; time-dependent dispersion.

1. Introduction

Solute transport in heterogeneous aquifers is a topic of great interest in subsurface hydrology since past few decades [1, 2]. Transport processes which govern the solute transport behavior within heterogeneous porous media are advection, dispersion, diffusion, sorption, and degradation [3–5]. Among these processes, dispersion plays an important role in deciding the dilution and mixing of solute in heterogeneous porous media [6–8]. Modelling solute transport through heterogeneous porous media is a complex process. Numerical simulation of solute breakthrough curve at one particular location cannot explain the overall plume evolution within porous media [4, 9–11]. On the other hand, moment analysis of solute concentrations is known as a potent tool to interpret solute behavior in heterogeneous porous media and therefore, widely used [4, 12]. Moment analysis has been used as an inverse modelling tool for estimating the solute transport parameters viz., effective solute velocity, effective dispersivity, and macro dispersion coefficient [10, 12, 13]. Temporal moments of solute concentrations are physically meaningful descriptors of solute breakthrough curves and have been used in several studies to elucidate the influence of transport parameters on solute transport and mixing mechanisms in porous media [9, 14, 15]. These moments provide a better description of the scale-dependency of lumped parameters used in governing equation of solute transport [16]. The zeroth temporal moment represents the mass of solute recovered at sampling point, first temporal moment describes the average residence time at a particular location, and second moment describes the degree of spreading about mean [17, 18]. Valocchi [19] used moment analysis for comparing simulation capabilities of different solute transport models and stated that temporal moments are very useful in analyzing sorbing solutes in one-dimensional system such as laboratory-scale columns. Several researchers performed a sensitivity analysis of various transport parameters using temporal moments to study plume evolution within porous media [9, 11, 20]. Renu and Kumar [14, 21] applied temporal moment analysis to investigate the influence of transport parameters (fracture aperture thickness, diffusion coefficient, fracture-skin porosity) on solute behavior in a fracture skin-matrix system. Sharma *et al* [9] analyzed

*For correspondence
Published online: 18 June 2020

transport characteristics using temporal moments in the fracture system. Suresh Kumar [16] concluded that the temporal moment analysis would give a better description of concentration distribution in the fracture system, having extended tailing portion in the BTC. However, time-dependent dispersion function has been considered in a few studies to understand the solute transport behavior in heterogeneous porous media [22–27]. Most of these studies focused on analytical and numerical results related to hypothetical problems. In these studies, observed experimental data had not considered in simulating solute transport through heterogeneous porous media. In several studies stated above, simulation capabilities of solute transport models have been identified only using breakthrough curve analysis.

In this study, the objective of temporal moment analysis is to determine lower-order time moments of solute concentration, therefore yielding significant physical insight of time-dependent dispersion function in the solute transport model. Firstly, effect of different variants of advection-dispersion model and mobile–immobile model on temporal moments of solute concentrations is studied. Then, solute velocity and macrodispersion coefficient are calculated using normalized temporal moments for various solute transport models. Further, we discuss the effect of mass-transfer coefficient, time-dependent dispersion coefficients, porewater velocity, and porosity of mobile region on solute transport in heterogeneous porous media using temporal moment analysis.

2. Governing equations

The mobile–immobile (MIM) model developed on the basis of two-region model, is used in this study [28, 29]. Advection, hydrodynamic dispersion in the mobile region, and first-order lumped mass transfer between mobile and immobile regions is considered for immobile region as done in the study by Guleria *et al* [30]. First-order decay on specific sites is considered for both the regions of porous media. Assuming linear sorption isotherm for the sake of simplicity, following governing equations can be written as:

$$(\theta_m + f\rho_b K_{d_m})\frac{\partial C_m}{\partial t} = \theta_m D_{(t)}\frac{\partial^2 C_m}{\partial x^2} - v_m\theta_m\frac{\partial C_m}{\partial x} - \omega(C_m - C_{im}) - (\theta_m\mu_{lm} + f\rho_b K_{d_m}\mu_{sm})C_m \quad (1)$$

$$(\theta_{im} + (1-f)\rho_b K_{d_{im}})\frac{\partial C_{im}}{\partial t} = \omega(C_m - C_{im}) - (\theta_{im}\mu_{\lim} + (1-f)\rho_b K_{d_{im}}\mu_{sim})C_{im} \quad (2)$$

where C_m and C_{im} are the solute concentrations in the mobile and immobile regions (M/L^3) at any time t respectively; x = spatial coordinate (L) taken in the direction of the fluid flow; $D_{(t)}$ represent time-dependent hydrodynamic dispersion coefficient along the flow velocity (L^2/T); θ_m and θ_{im} are volumetric water contents of the mobile and immobile regions respectively; v_m = mobile pore water velocity (L/T); $v_m\theta_m$ is equal to q(flow rate (L/T)); ω is the first order mass transfer coefficient (/T); f and $(1-f)$ represent the fractions of sorption sites that equilibrate instantly with the mobile and immobile regions, respectively; μ_{lm} and $\mu_{\lim}$ are the first-order decay coefficients for degradation of solutes in the mobile and immobile solution phases respectively; μ_{sm} and μ_{sim} are the first-order decay coefficients for degradation of solutes in the mobile and immobile region adsorbed solid phases respectively; K_{dm} = distribution coefficient of linear sorption process (L^3/M) in the mobile region; K_{dim} = distribution coefficient of linear sorption process (L^3/M) in the immobile region; ρ_b = bulk density of the porous medium (M/L^3).

In this study, a linear and asymptotic form of time-dependent dispersion is considered with mobile–immobile model (MIM) to compute the breakthrough curves (BTCs) at various down-gradient location firstly as done in the published work by Guleria *et al* [30]. Further, moments of solute concentration are calculated to interpret the solute behavior. We define following abbreviations to represent our results: MIML is the mobile–immobile model with a linear time-dependent dispersion parameter. MIMA is the mobile–immobile model with asymptotic time-dependent dispersion parameter [30].

Linear time-dependent dispersion function:

$$D_{(t)} = D_0\frac{t}{K_L} + D_m \quad (3a)$$

Asymptotic time-dependent dispersion function:

$$D_{(t)} = D_0\frac{t}{t + K_A} + D_m \quad (3b)$$

Where D_0 = maximum dispersion coefficient (L^2/T) for asymptotic time-dependent dispersion function and uniform dispersion coefficient for linear time-dependent dispersion function respectively; D_m= effective diffusion coefficient (L^2/T); t = time (T); K_A(T) is the asymptotic time-dependent dispersion coefficient which is equivalent to mean travel time; K_L(T)is the linear time-dependent dispersion coefficient.

2.1 *Initial condition*

The initial condition assumes that the porous medium is not contaminated and is given as follows:

$$C_m(x,0) = C_{im}(x,0) = 0 \quad (4)$$

2.2 *Boundary conditions*

Dirichlet type boundary condition at inlet – Continuous source concentration

$$C_m(0,t) = C_0 \tag{5a}$$

Dirichlet type boundary condition at inlet – Pulse type source concentration

$$C_m(0,t) = \begin{cases} C_0, & 0 < t \le t_p \\ 0, & t > t_p \end{cases} \tag{5b}$$

Neumann type boundary condition at the outlet

$$\left(\frac{\partial C_m(x,t)}{\partial x}\right)_{(x=L,t)} = 0 \tag{6}$$

Where $C_0 =$ injected concentration (M/L^3) of solute source at the inlet of the porous medium. Dirichlet type (eq. (5)) boundary condition is considered at inlet. However, Neumann type (eq. (6)) boundary condition is assumed at outlet which preserves concentration continuity for a semi-infinite system.

3. Numerical solution and moment analysis

In the present model, solute transport through saturated porous media is described by coupled partial differential equations in 1-D domain. A finite-difference numerical method utilizing the Crank-Nicolson technique has been employed to obtain the solution of the mobile–immobile (MIM) transport equation with arbitrary time-dependent dispersion. Details of the spatial discretization adopted are shown in the previous work carried out by Guleria *et al* [30]. Discretized form of solute transport equations in the mobile–immobile domain is presented below:

$$\begin{aligned} R_m\left(\frac{C_{mi}^{t+1} - C_{mi}^{t}}{\Delta t}\right) &= \frac{\theta_m D_{(t+1)}}{2}\left(\frac{C_{mi+1}^{t+1} - 2C_{mi}^{t+1} + C_{mi-1}^{t+1}}{\Delta x^2}\right) \\ &+ \frac{\theta_m D_{(t)}}{2}\left(\frac{C_{mi+1} - 2C_{mi}^{t} + C_{mi-1}^{t}}{\Delta x^2}\right) \\ &- \frac{\theta_m v_m}{2}\left(\frac{C_{mi}^{t+1} - C_{mi-1}^{t+1}}{\Delta x}\right) \\ &- \frac{\theta_m v_m}{2}\left(\frac{C_{mi}^{t} - C_{mi-1}^{t}}{\Delta x}\right) \\ &- \frac{\omega}{2}\left(C_{mi}^{t+1} - C_{imi}^{t+1}\right) - \frac{\omega}{2}\left(C_{mi}^{t} - C_{imi}^{t}\right) \\ &- \frac{A_1}{2}C_{mi}^{t+1} - \frac{A_1}{2}C_{mi}^{t} \end{aligned} \tag{7}$$

$$\begin{aligned} R_{im}\left(\frac{C_{imi}^{t+1} - C_{imi}^{t}}{\Delta t}\right) &= \frac{\omega}{2}\left(C_{mi}^{t+1} - C_{imi}^{t+1}\right) + \frac{\omega}{2}\left(C_{mi}^{t} - C_{imi}^{t}\right) \\ &- \frac{A_2}{2}C_{imi}^{t+1} - \frac{A_2}{2}C_{imi}^{t} \end{aligned} \tag{8}$$

where

$$R_m = (\theta_m + f\rho_b K_{dm}) \tag{9a}$$

$$R_{im} = (\theta_{im} + (1-f)\rho_b K_{dim}) \tag{9b}$$

$$A_1 = (\theta_m \mu_{lm} + f\rho_b K_{dm}\mu_{sm}) \tag{9c}$$

$$A_2 = \left(\theta_{im}\mu_{\lim} + (1-f)\rho_b K_{dim}\mu_{sim}\right) \tag{9d}$$

where, $\Delta t =$ time step; $\Delta x =$ grid size; t denotes the known time and $(t+1)$ denotes the unknown time level.

$$\begin{aligned} &A_7 C_{mi}^{t+1} - \left(A_3 D_{(t+1)}\right)C_{mi+1}^{t+1} - \left(A_3 D_{(t+1)} + A_4\right)C_{mi-1}^{t+1} - A_5 C_{imi}^{t+1} \\ &= A_{10} C_{mi}^{t} + \left(A_3 D_{(t)}\right)C_{mi+1}^{t} + \left(A_3 D_{(t)} + A_4\right)C_{mi-1}^{t} + A_5 C_{imi}^{t} \end{aligned} \tag{10}$$

$$A_8 C_{imi}^{t+1} - A_9 C_{mi}^{t+1} = A_{11} C_{imi}^{t} + A_9 C_{mi}^{t} \tag{11}$$

Where coefficients are defined below:

$$A_3 = \frac{\theta_m}{\Delta x^2}\left(\frac{\Delta t}{2R_m}\right),\ A_4 = \frac{v_m \theta_m}{\Delta x}\left(\frac{\Delta t}{2R_m}\right)$$

$$A_5 = \frac{\omega \Delta t}{2R_m}, A_6 = \frac{A_1 \Delta t}{2R_m}$$

$$A_7 = 1 + \left(2A_3 D_{(t+1)}\right) + A_4 + A_5 + A_6$$

$$A_8 = 1 + \left(\frac{\omega \Delta t}{2R_{im}}\right) + \left(\frac{A_2 \Delta t}{2R_{im}}\right), A_9 = \left(\frac{\omega \Delta t}{2R_{im}}\right)$$

$$\begin{aligned} A_{10} &= 1 - \left(2A_3 D_{(t)}\right) - A_4 - A_5 - A_6, A_{11} \\ &= 1 - \left(\frac{\omega \Delta t}{2R_{im}}\right) - \left(\frac{A_2 \Delta t}{2R_{im}}\right) \end{aligned}$$

$D_{(t)}$ is the time-dependent dispersion coefficient which is updated after each time step in the numerical simulation. Steps involved in the solution algorithm are described below.

1. The value of C_{imi}^{t+1} obtained from equation (11) has been substituted in equation (10) so that the resulting expression contains mobile region $\left(C_{mi}^{t+1}\right)$ concentration for the unknown time level and mobile and immobile region concentrations for the known time level. The obtained equation is then solved using the tridiagonal matrix algorithm (Thomas algorithm) to get C_{mi}^{t+1} for all the nodes.
2. The computed value of C_{mi}^{t+1} is then substituted in equation (11) to get the values of immobile region concentration for unknown time level C_{imi}^{t+1} at all the nodes.
3. Finally, updating of C_{mi}, C_{imi}, and $D_{(t)}$ has been done before going to next time level.
4. Steps 1-3 are repeated for the next time level and simulation ends when total simulation time is reached.

3.1 *Calculation of temporal moments*

Temporal moment of solute concentration represents the time-averaged solute behavior within porous media [17].

The *n*th order absolute temporal moment of a breakthrough curve (BTC) at a location x, is defined as:

$$M_n = \int_0^T t^n C(x,t)dt \tag{12}$$

where for $n = 0, 1, 2$, obtained moments M_0, M_1, and M_2 represents zeroth, first, and second absolute temporal moments respectively and T is the total resident time. *n*th order normalized temporal moment is given by following equations:

$$\mu_n = \frac{M_n}{M_0} = \frac{\int_0^T t^n C(x,t)dt}{\int_0^T C(x,t)dt} \tag{13}$$

$$T_1(x) = \mu_1 \tag{14}$$

$$T_2(x) = \mu_2 - (\mu_1)^2 \tag{15}$$

where μ_1, and μ_2 are the normalized first, and second temporal moments respectively. $T_1(x)$ and $T_2(x)$ are the first temporal moment and second temporal moments, respectively.

Normalization in Equation (13) is done to determine transport properties and distribution behavior of solute within porous media. Moments describe the central tendency of probability distributions. Of n possible moments, the first four are frequently used to describe the central tendency of distribution [17]. These first four moments correspond to the total mass density, arithmetic mean, variance, and skewness of the distribution. Once the probability distributions are established, then the statistical properties of moments may be applied to study solute transport simply by replacing X with a time variable and $P(X)$ with relative concentration [17]. In principle, the relative concentration C equals the probability density f and is defined as the ratio between concentrations measured in effluent at a given time and the cumulative concentration recovered in effluent during a leaching experiment [17]. First temporal moment $(T_1(x))$ is the descriptor of mean residence time, which is average time spend by solute molecules inside the porous media. Second central temporal moment $(T_2(x))$ represents the variance of the BTC, which provides a measure of solute spreading [11, 17, 30].

Solute velocity and macro-dispersion coefficient can be obtained using computed first and second normalized temporal moments of solute concentrations, as explained in the following expressions [14, 17, 20, 21]:

$$V(x) = \frac{dx}{d\{T_1(x)\}} \tag{16}$$

$$D_{macro}(x) = \frac{1}{2}\frac{V^3 d\{T_2(x)\}}{dx} \tag{17}$$

where $V(x)$ and $D_{macro}(x)$ represent the solute velocity and macro-dispersion coefficient respectively in the porous media corresponding to a particular location (x) in the longitudinal direction.

Equations of normalized temporal moments (Eqs. (14) and (15)) are valid for concentration pulse source [9, 17, 21]. A first derivative of the concentration in the porous media is used to obtain the equivalent pulse of constant continuous source used at the inlet in order to use Eqs. (12) to (15) [9, 17, 21].

4. Validation of the numerical model

There is no analytical solution available for mobile–immobile model with time-dependent dispersion. Therefore, numerical solution was validated for simpler case by scaling down mobile–immobile model to advection-dispersion model. Firstly, presented numerical solution was validated with the analytical solution of 1-D advection-dispersion equation with time-dependent dispersion developed by Basha and El-Habel [27]. The detailed description of initial condition, boundary conditions and input parameters is presented in the study by Guleria *et al* [30]. By keeping the value of mass-transfer coefficient $(\omega) = 0$ and porosity of immobile region = 0, MIMA model transformed to advection-dispersion equation with asymptotic time-dependent dispersion. For validation, following input parameters are used: L= 100 m, saturated porosity (θ) =0.35, mass-transfer coefficient $(\omega) = 0$, pore-water velocity (v_m) = 0.25 m/day, retardation factor $(R) = 1$, total time = 200 days, bulk density (ρ_b) = 2.11 gm/cm^3, maximum dispersion coefficient (D_0) = 1 m^2/day, asymptotic time-dependent dispersion coefficient (K_A) = 50 days, effective molecular diffusion coefficient (D_m) = 0 m^2/day, first order decay constant =0 day^{-1}. The grid size and time step are taken by keeping Peclet number, $Pe < 2$ and Courant number, $Cr < 1$ [31].

It is observed that the numerical solutions show good agreement with results obtained from Basha and El-Habel [27] as presented in figure 1. In the second validation case, numerical solution was validated with the analytical solution of convection-dispersion model developed by Barry and Sposito [25]. Continuous source boundary condition is assumed at the position $x = 0$. In this case, MIMA model transformed to advection-dispersion equation with constant dispersion by neglecting the value of mass-transfer coefficient (ω), saturated porosity of immobile region, and asymptotic time-dependent dispersion coefficient (K_A). Input parameters used in validation are as follows: $L = 5$ cm, pore-water velocity (v_m) = 1 cm/day, retardation factor $(R) = 1$, total time = 2.5 days, maximum dispersion coefficient (D_0) = 0.05 cm^2/day, effective molecular diffusion coefficient (D_m) = 0 m^2/day, and first-orderr decay constant = 0 day^{-1}.

Numerical solution matches well with the analytical solution obtained by Barry and Sposito [25] as presented by spatial variation of C/C_0 at $T = 2.5$ days (figure 2).

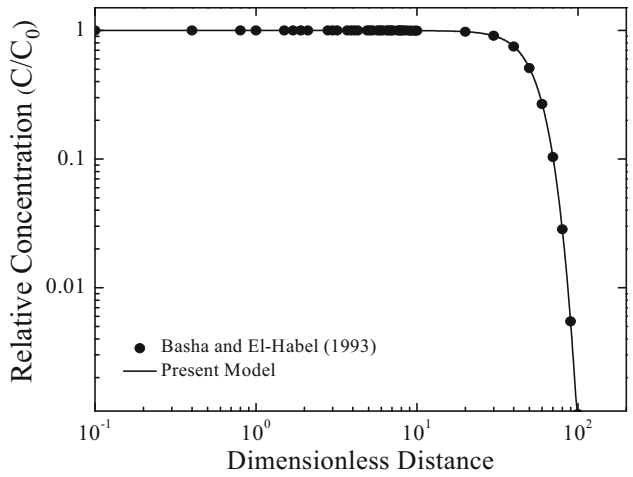

Figure 1. Concentration profile for non-reactive solute at time, T = 200 days.

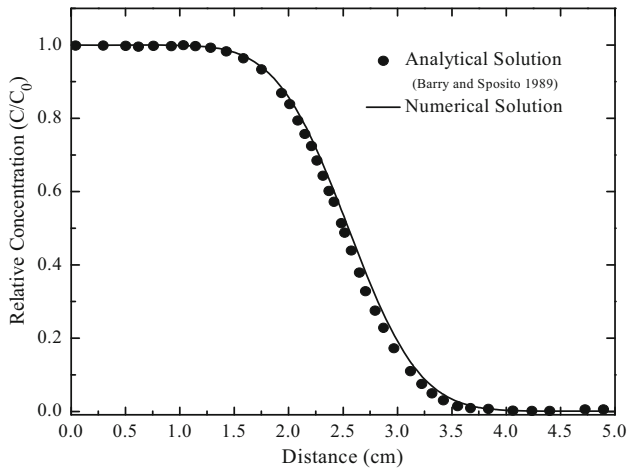

Figure 2. Spatial concentration profile for non-reactive solute at time, T = 2.5 days.

5. Results and discussions

Simulation of observed experimental BTCs using various transport models is a prerequisite for comparison of models using temporal moments. Firstly, constant (MIMC) and time-dependent dispersion models (MIML and MIMA) are used to simulate observed experimental BTCs of chloride transport in stratified porous media. BTC data of chloride obtained at 400 cm down-gradient distance is taken from Swami *et al* [32], and also, simulation of BTC is presented in study by Guleria *et al* [30]. There are two parameters (ω, D_0) in mobile–immobile model with constant dispersion (MIMC) and three parameters $(\omega, D_0, K_A or K_L)$ in the linear time-dependent dispersion model (MIML) and asymptotic time-dependent dispersion model (MIMA) which need to be estimated using inverse procedure at 400 cm down-gradient distance. MIMC, MIML, and MIMA have similar θ_m and v_m. Pulse type boundary condition is considered at inlet. Maximum simulation time (t) = 10080 minute, pulse duration (t_p) = 2880 minute, L = 400 cm, q = 0.04 cm/min, θ_m= 0.33, θ_{im}= 0.42, mobile-water fraction (f) = 0.44, v_m= 0.121 cm/min have been used for simulation [30]. Estimated values of parameters for MIMC, MIML and MIMA are presented in table 1.

Simulation of BTC of chloride transport using MIMC, MIML, and MIMA model for 400 cm down-gradient distance is shown in figure 3. Log-log plot has been used to represent low-concentration data and to show the simulation capabilities of different dispersion models. After simulating BTC at down-gradient location, comparison of models and sensitivity analysis has been carried out as shown in the below sections.

5.1 *Effect of conceptual model on temporal moments of solute concentration*

In order to analyze the simulation capabilities of different solute transport models, temporal moment analysis of solute concentrations was conducted. Five different solute transport models were considered. These are: (1) advection-dispersion model with linear time-dependent dispersion (ADEL), (2) advection-dispersion model with asymptotic time-dependent dispersion (ADEA), (3) mobile–immobile model with constant dispersion (MIMC), (4) mobile–immobile model with linear time-dependent dispersion (MIML), and (5) mobile–immobile model with asymptotic time-dependent dispersion (MIMA). In this section, domain length is exaggerated from 400 cm to 3000 cm to investigate the effect of conceptual model on solute transport at larger scale (i.e., 30 m). Pulse type source boundary condition is considered at inlet. Maximum simulation time (t) = 10080 minute, pulse duration (t_p) = 2880 minute, L = 3000 cm, q = 0.04 cm/min, θ_m= 0.33, θ_{im}= 0.42, mobile-water fraction (f) = 0.44, v_m= 0.121 cm/min have been used for simulation. Transport parameters of dispersion model used in the analysis are shown in table 1. For ADEL and ADEA models, the value of mass-transfer coefficient (ω) and porosity of immobile region (θ_{im}) are kept zero, while other parameters are kept same as for the MIML and MIMA models.

Figure 4(a) compares the spatial distribution of zeroth temporal moment (solute mass recovery) for different solute transport models. It is evident that the solute mass recovery decreases with travel distance for all the models. It is observed that the value of zeroth temporal moment is highest for MIMC model as compared to MIML and MIMA model up to 400 cm travel distance. Solute mass recovery for MIMC model decreases with travel distance (up to 400 cm) at constant rate. However, at short travel distances (up to 400 cm), solute mass recovery for MIMA model decreases at mild slope as compared to MIMC and MIML. At large travel distances (after 1000 cm), solute mass recovery for MIMC model is lower than MIML and

Table 1. Estimated parameters used for comparison of dispersion models.

Parameter	Value	Parameter	Value
D_0(MIMC)	2.51 cm^2/min	D_0 (MIMA)	4.51 cm^2/min
Mass-transfer coefficient, ω (MIMC)	3.12E-05 min^{-1}	K_A (MIMA)	200 min
D_0 (MIML)	5.89 cm^2/min	Mass-transfer coefficient, ω (MIMA and MIML)	2.12E-05 min^{-1}
K_L (MIML)	4500 min		

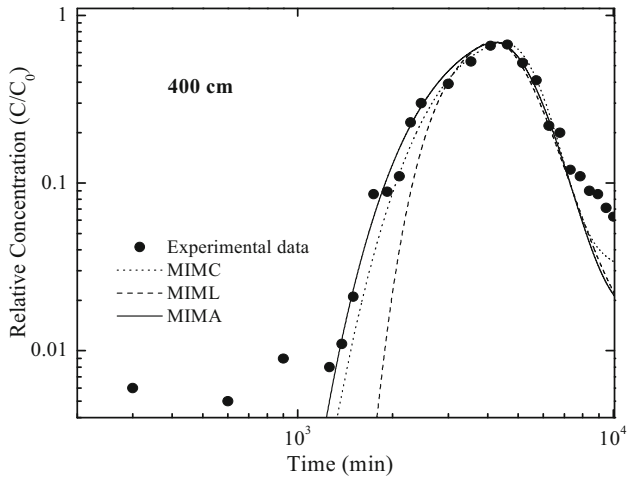

Figure 3. Simulation of experimental breakthrough curve of chloride at 400 cm down-gradient distance for v_m = 0.121 cm/min using different dispersion models.

MIMA models due to single lumped value of dispersion coefficient for entire simulation period whereas for time-dependent models (MIML, MIMA), dispersion coefficient changes with simulation time. Solute mass recovery is observed to be lower for mobile–immobile model (MIMC, MIML, and MIMA) as compared to advection-dispersion model (ADEL, ADEA) as a result of mass transfer from mobile to the immobile region within the porous media as shown in figure 4 (a). Zeroth temporal moment for ADEL and MIML models decreases with travel distance upto 400 cm at a uniform steep slope due to linear variation of effective dispersion coefficient with time. However, solute mass recovery for ADEA and MIMA models decreases at mild slope upto 400 cm travel distances. Further, spatial variation of first temporal moment (mean arrival time) of solute for different solute transport models is shown in figure 4(b). Linear variation of mean arrival time with travel distance is observed upto 300 cm from inlet source and asymptotic value is found at larger travel distance. The magnitude and trend of mean arrival time approximately remains the same for ADEL, ADEA, MIML and MIMA models. The value of first temporal moment is highest for MIMC model during whole simulation period due to single lumped value of dispersion coefficient. It can be concluded that MIMC simulates transport behavior for smaller distances or experimental duration, however, fails to represent plume behavior at field-scale condition.

Figure 4(c) shows the spatial variation of second temporal moment for different solute transport models i.e., ADEL, ADEA, MIMC, MIML, and MIMA. The second temporal moment increases with travel distance at faster rate due to proximity to source point and attains a peak value and then decreases non-uniformly at gradual slope with travel distance for all the considered models. The second temporal moment for MIML model is observed as highest in comparison to other solute transport models (ADEL, ADEA, MIMC and MIMA) which may be due to linear dependency of dispersion function on simulation time without any upper bound. At large travel distances (after 1000 cm), second temporal moment becomes almost same for all the time-dependent solute transport models (i.e., ADEL, ADEA, MIML, and MIMA) and attains an asymptotic value which represent the complete dilution of source concentration. It is observed that the value of second temporal moment is different for MIMC model as compared to time-dependent solute transport models which is due to single lumped value of dispersion coefficient for entire simulation length and time. The peak value of second temporal moment is higher for mobile–immobile models (MIML and MIMA) than the advection-dispersion models (ADEL and ADEA). It can be concluded that the physical non-equilibrium transport behavior dominates the dispersion of solute in heterogeneous porous media.

Solute velocity and macrodispersion coefficient can be computed from the slope of first temporal moment and second temporal moment respectively as described in equations (16) and (17). Figure 5(a) presents the computed solute velocity in the porous media for different solute transport models. Less variation in the computed solute velocity (i.e., from 0.08 cm/min to 0.13 cm/min) is observed up to 300 cm travel distance as shown in figure 5(a). It implies solute velocity remains constant and solute mobility is not scale-dependent up to 300 cm travel distance. Computed solute velocity is observed to be highest for MIMC model in comparison to MIML and MIMA model after 1200 cm which may be due to single lumped value of dispersion coefficient considered during whole simulation length and time.

Variation of macrodispersion coefficient for different solute transport models is presented in figure 5(b). Macrodispersion coefficient computed for MIMC model varies linearly with travel distance which represents the effect of constant dispersion function in simulation model. On the other hand, non-linear variation of computed

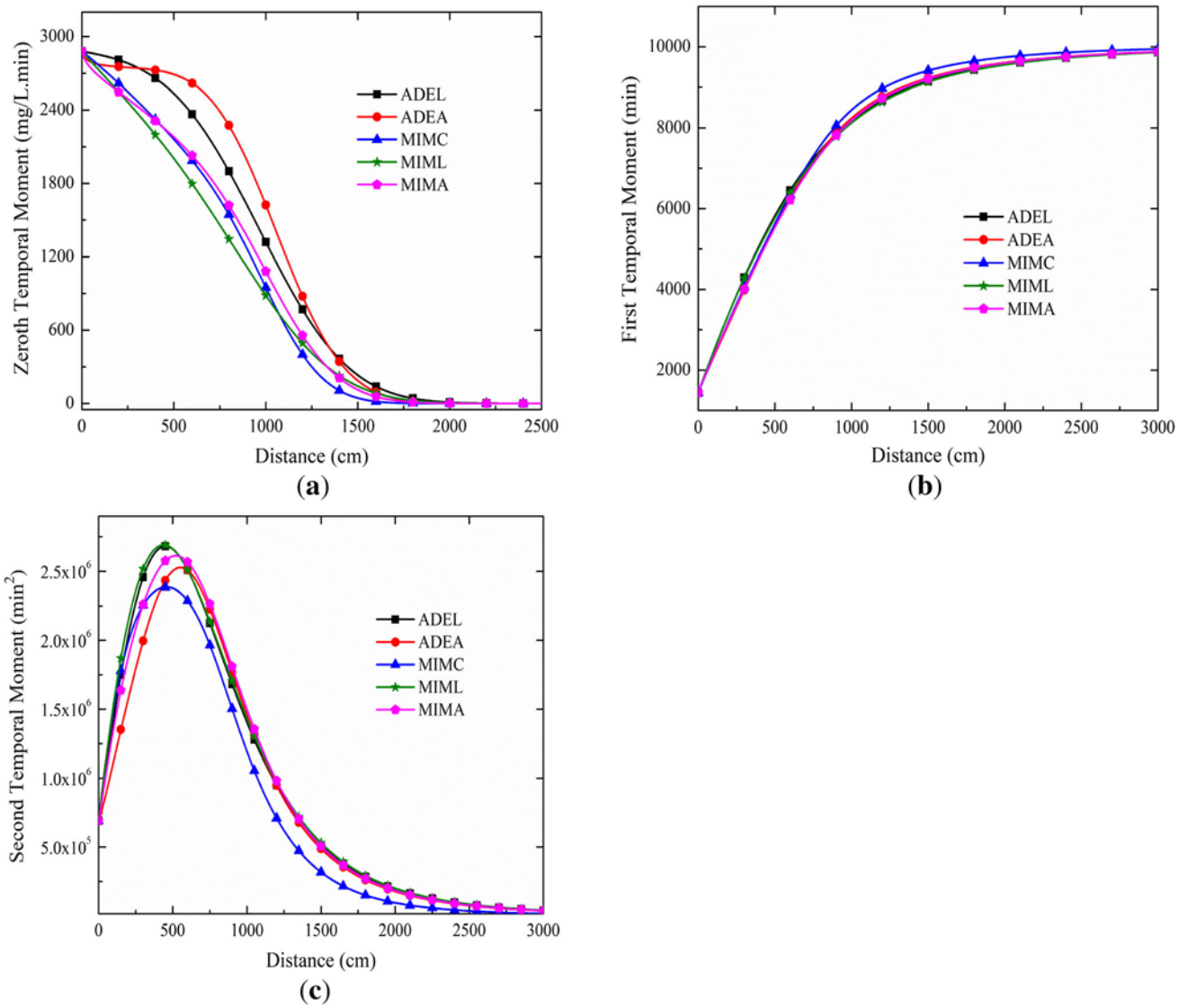

Figure 4. Effect of conceptual model on (**a**) zeroth, (**b**) first, and (**c**) second temporal moment of solute concentration.

macrodispersion coefficient is observed for all the time-dependent dispersion-based models (ADEA, ADEL, MIML, MIMA). It indicates that the magnitude of macrodispersion coefficient is scale-dependent and solute transport behavior through heterogeneous porous media can be better captured by time-dependent dispersion function. In the next section, sensitivity analysis of transport parameters is discussed which yield physical insight into the behavior of solute transport through heterogeneous porous media with time-dependent dispersion.

5.2 *Sensitivity analysis of time-dependent transport parameters*

5.2a *Effect of porewater velocity:* Advection and dispersion processes are majorly influenced by porewater velocity within porous media. Therefore, in this section, influence of porewater velocity on plume evolution is investigated using temporal moments of solute concentration. Porewater velocity (v_m) is varied as 0.10 cm/min, 0.20 cm/min, and 0.50 cm/min while keeping other transport parameters (ω = 2.12E-05 min^{-1}, K_A = 200) fixed. Figure 6(a) shows the spatial variation of zeroth temporal moment of solute concentration (M_0) for different values of porewater velocity (v_m). Solute mass recovery at particular location increases with an increase in porewater velocity (v_m). This may be due to the dominance of advection over dispersion process due to which higher amount of solute mass is recovered with an increase in porewater velocity. Solute mass recovery varies inversely with travel distance and slope of the profile becomes flatter with increasing porewater velocity (v_m).

Spatial variation of first temporal moment of solute concentration for different values of porewater velocity

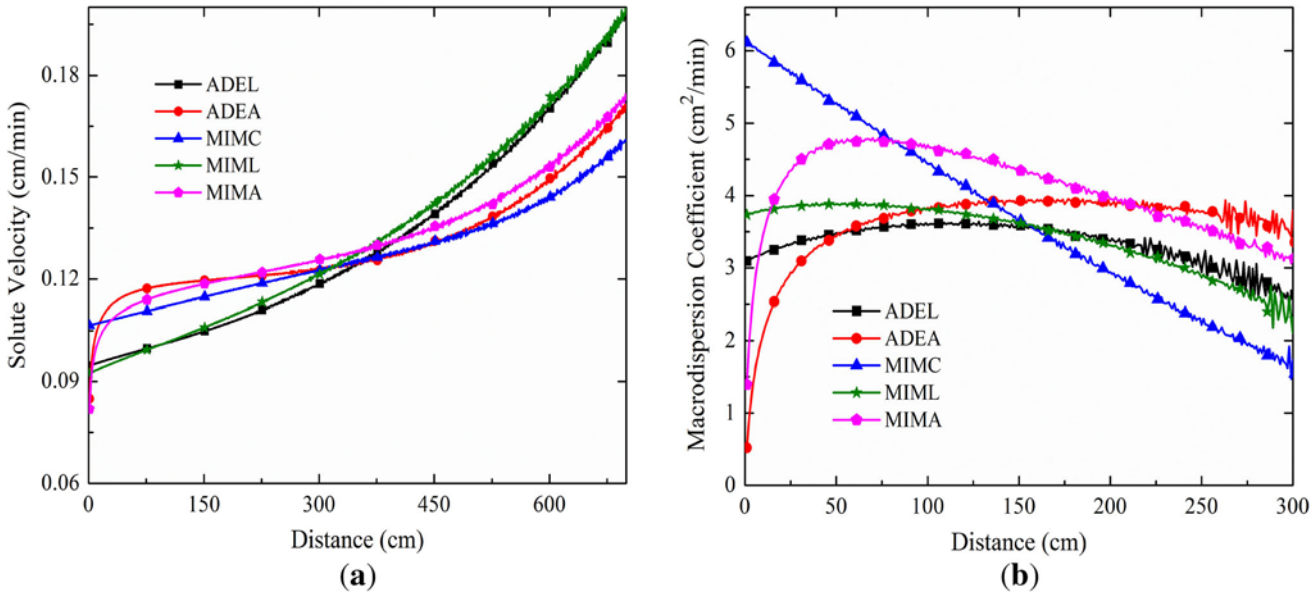

Figure 5. (**a**) Solute velocity and (**b**) macrodispersion coefficient as a function of travel distance (cm) for different solute transport model.

(v_m) is shown in figure 6(b). It is observed that the average residence time of solute decreases with an increase in porewater velocity (v_m). Since solute is advected forward with higher porewater velocity and remain in the porous system for lesser duration which cause lower value of first temporal moment at higher porewater velocity. First temporal moment increases linearly with travel distance and slope of the profile decreases with increasing porewater velocity. Variation of second temporal moment of solute concentration (M_0) with travel distance for different values of porewater velocity (v_m) is shown in figure 6(c). Non-linear variation of second temporal moment with travel distance is observed at lower porewater velocity ($v_m = 0.10$ cm/min). While, second temporal moment varies linearly with travel distance at higher pore water velocity. Since, dominance of dispersion over advection decreases with an increase in porewater velocity. Due to this, dispersion varies gradually and cause non-uniform variation of second temporal moment.

5.2b *Effect of porosity of mobile region*: The influence of porosity of mobile region on plume behavior in heterogeneous porous media is studied using temporal moments of solute concentration. θ_m is varied as 0.23, 0.33, and 0.43, while other transport parameters are kept fixed to their respective values. Figure 7(a) shows the spatial variation of zeroth temporal moment of solute concentration (M_0) for different values of porosity of mobile region. As porewater velocity ($v_m = q/\theta_m$) is inversely related to porosity of mobile region, so increase in θ_m value leads to decrease in porewater velocity. Therefore, solute mass recovery at particular location decreases with an increase in porosity of mobile region (θ_m). Spatial variation of first temporal moment for different values of porosity of mobile region is shown in figure 7(b). It is observed that the first temporal moment increases linearly with travel distance and slope of the profile become steeper with an increase in porosity of mobile region. It is observed that the average residence time of solute increases with an increase in porosity of

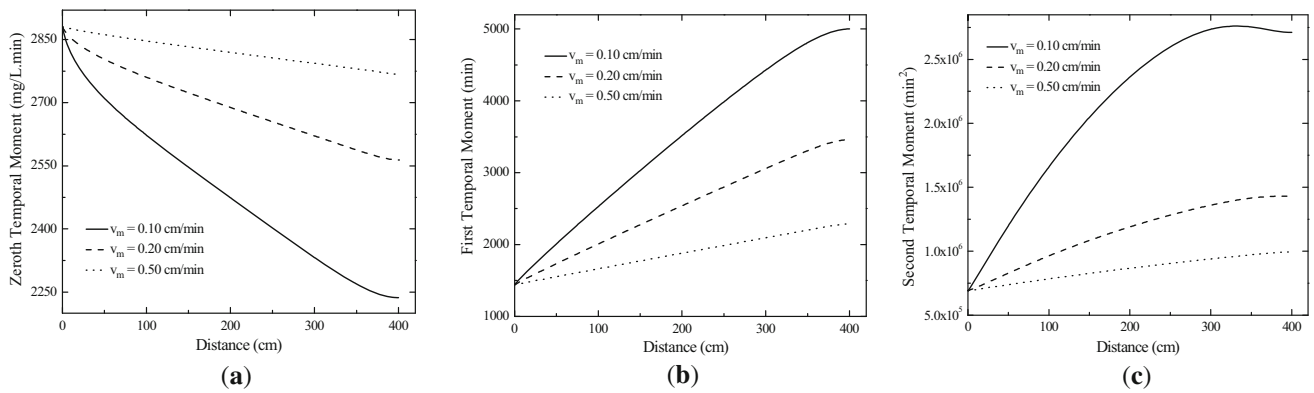

Figure 6. Effect of pore-water velocity on (**a**) zeroth, (**b**) first, and (**c**) second temporal moment of solute concentration.

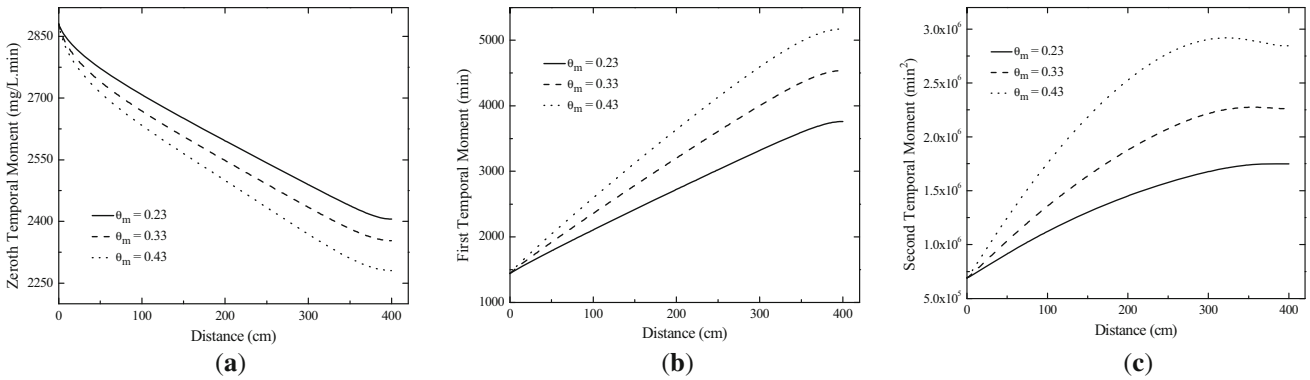

Figure 7. Effect of porosity of mobile region on (**a**) zeroth, (**b**) first, and (**c**) second temporal moment of solute concentration.

mobile region (θ_m). This may be caused due to the decrease in porewater velocity and thus, increase in pore water area. As these factors slow down the dilution of plume by dispersion processes and solute remain in the porous system for longer time, which lead to increase in average residence time of solute. Figure7(c) shows the spatial distribution of second temporal moment of solute concentration (M_0) for different values of porosity of mobile region (θ_m). Second temporal moment is found as non-linearly varying with travel distance and the slope of the profile increases with the travel distance and finally, approaches zero value at later distances. Also, direct dependency of second temporal moment upon porosity of mobile region (θ_m) is observed.

5.2c *Effect of mass-transfer coefficient:* Anomalous transport behavior of solute in saturated porous media is related to physical and chemical partitioning. Physical partitioning (non-equilibrium) behavior appeared due to hydraulic coupling between different porous media layers having different hydraulic conductivities. Mathematically, mass transfer coefficient represents diffusive mass flux transfer in such type of porous systems (i.e., stratified porous media in which one layer behaves as sink/source component). For non-reactive solute, mass-transfer coefficient plays major role in anomalous transport behavior through heterogenous porous media. Therefore, in this section, effect of mass-transfer coefficient on plume evolution is analyzed using temporal moments of solute concentration. Mass transfer coefficient (ω) is varied from 2.12E-06 min^{-1} to 2.12E-04 min^{-1} as diffusion coefficient of several solutes vary over wide range. Zeroth temporal moment decreases with an increase in mass transfer coefficient (ω) as shown in figure 8(a). It shows that an increase in the value of mass transfer coefficient (ω) decreases the solute concentration in the mobile region. Therefore, less solute mass is recovered at higher mass transfer coefficient (ω). It is observed that for lower value of mass-transfer coefficient (ω), less spatial variation of zeroth temporal moment occurred. However, for higher value of ω, large variation of zeroth temporal moment is observed along longitudinal distance. It may be due to large amount of solute mass transfer between mobile and immobile regions.

Spatial variation of first temporal moment (mean residence time) for different values of mass transfer coefficient (ω) is shown in figure 8(b). First temporal moment increases linearly with travel distance at lower values of mass-transfer coefficient ($\omega = 2.12 \times 10^{-6}$ min^{-1}), while non-linear variation with travel distance is observed at higher value of mass-transfer coefficient ($\omega = 2.12 \times 10^{-4}$ min^{-1}). Due to large amount of solute mass transfer from mobile to immobile region at higher mass-transfer coefficient ($\omega = 2.12 \times 10^{-4}$ min^{-1}), solute mass remains in the porous system for longer duration, and after source removal/isolation, stored mass in immobile regions transfer back to mobile region, causes enhancement of the residence time of solute within the porous media. Similarly, an increase in the first temporal moment is observed with an increase in mass-transfer coefficient.

Figure 8(c) shows the spatial distribution of second temporal moment for different values of mass-transfer coefficient (ω). Second temporal moment increases non-uniformly with travel distance at higher value of mass-transfer coefficient ($\omega = 2.12 \times 10^{-4}$ min^{-1}). While, slope of second temporal moment and travel distance is mild at lower values of mass-transfer coefficient ($\omega = 2.12 \times 10^{-6}$ min^{-1}). Due to large solute mass difference between mobile and immobile regions, solute mass may be eluded from immobile region at later travel time and travel distance which cause non-linear variation of second temporal moment at higher mass transfer coefficient.

5.2d *Effect of time-dependent dispersion coefficients D_0 and K_A of MIMA dispersion model:* The influence of asymptotic time-dependent dispersion parameters on plume behavior is studied using temporal moments. Following input parameters are used in the simulation to study the influence of dispersion coefficient: mass transfer coefficient (ω) = 2.12E-05 min^{-1}, L = 400 cm, K_A = 200, total simulation time = 10080 minutes, pulse duration of 2880 minutes, and D_0 value is varied from 1 cm^2/min to 10 cm^2/min. Figure 9(a) shows the spatial variation of zeroth temporal moment (M_0) for different values of dispersion

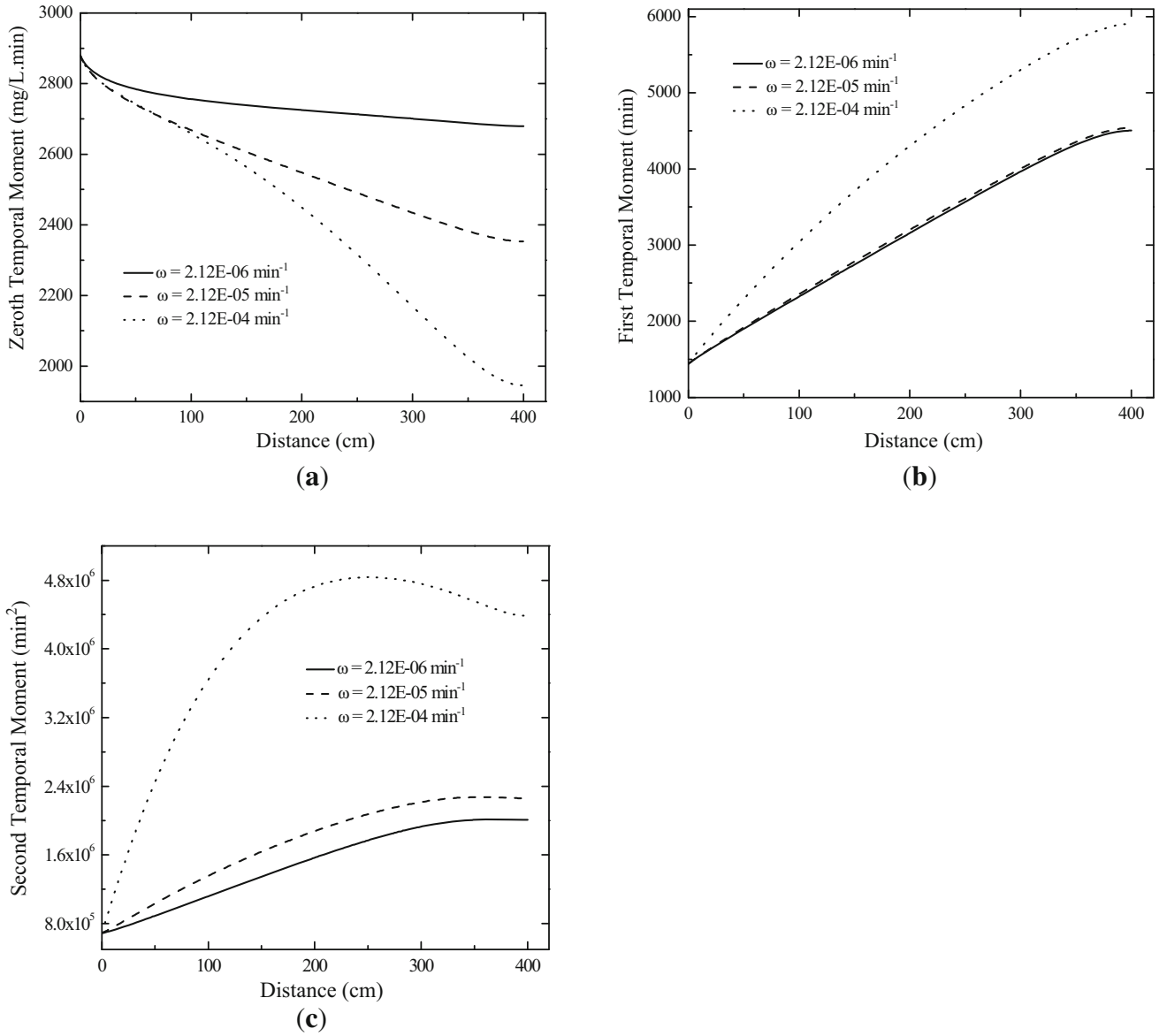

Figure 8. Effect of mass-transfer coefficient on (**a**) zeroth, (**b**) first, and (**c**) second temporal moment of solute concentration.

coefficient (D_0) of MIMA model. Solute mass recovery is lowest at 400 cm down-gradient distance due to location of point away from inlet source point. Zeroth temporal moment varies inversely with dispersion coefficient (D_0) of MIMA model. It indicates that an increase in the value of dispersion coefficient (D_0) reduces the solute mass in the mobile region. Spatial variation of mean residence time for different values of dispersion coefficient (D_0) of MIMA model is shown in figure 9 (b). The value of first temporal moment varies linearly for short travel distances, while non-linear variation is observed for larger travel distances. It is observed that mean residence time behaves independent of the dispersion coefficient (D_0) at short travel distances near to source. However, at later travel distances away from source, first temporal moment is lower for higher value of dispersion coefficient (D_0). This may be due to early appearance (breakthrough) of solute particles because of higher effective dispersion value. Figure 9(c) shows the spatial variation of second temporal moment for different values of dispersion coefficient (D_0) of MIMA model. The peak value of second temporal moment is highest for largest value of dispersion coefficient ($D_0 = 10\ \mathrm{cm}^2/\mathrm{min}$). It is also observed that the second temporal moment varies non-linearly with travel distance and the slope of the profile become flatter as the distance from the source increases and finally it reaches to zero value.

Furthermore, effect of mean travel time (K_A) of MIMA dispersion model on plume behavior is investigated using temporal moments by varying K_A from 0 min to 200 min. Figure 9(d) shows the spatial distribution of zeroth temporal moment (M_0) with K_A for MIMA model. The value of

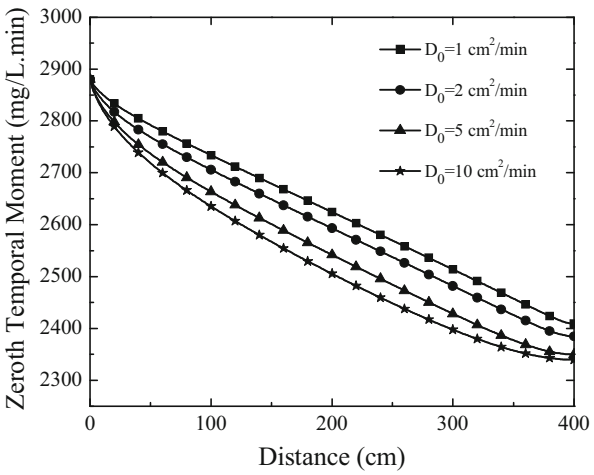

(**a**)

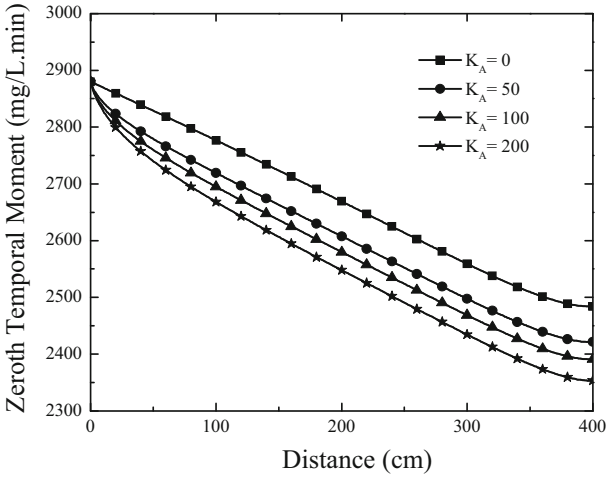

(**d**)

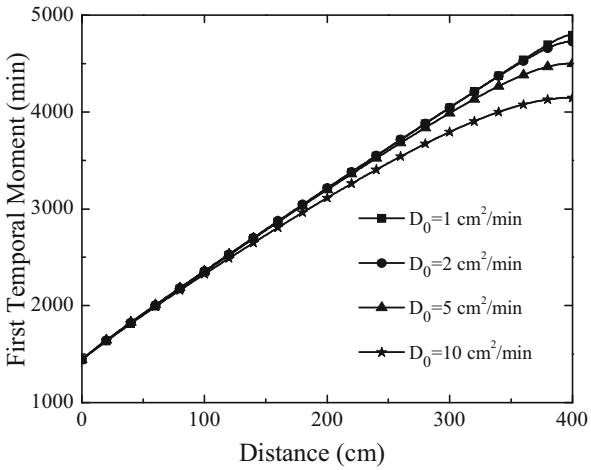

(**b**)

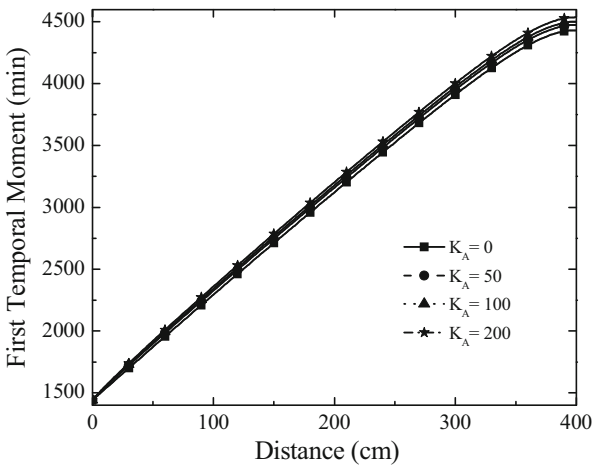

(**e**)

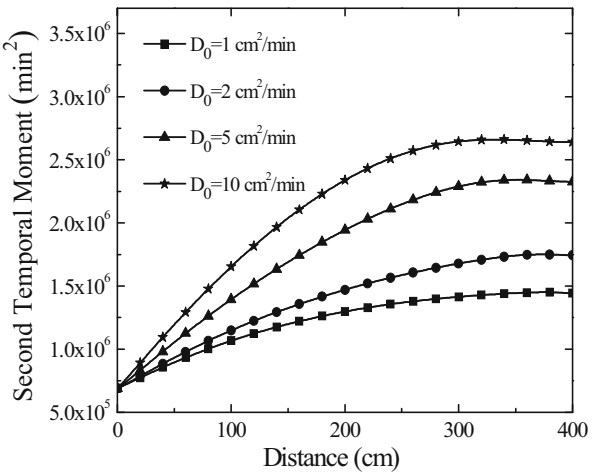

(**c**)

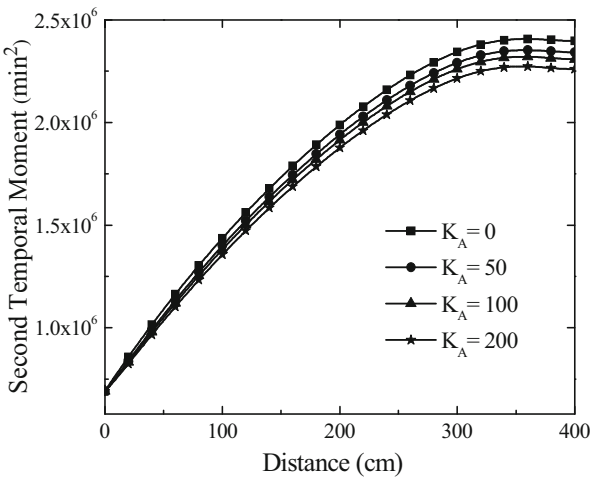

(**f**)

Figure 9. Effect of time-dependent dispersion coefficients D_0 (**a, b,** and **c**) and K_A (**d, e,** and **f**) of MIMA dispersion model on plume evolution: (**a** and **d**) zeroth moment of solute concentration; (**b** and **e**) first moment of solute concentration; (**c** and **f**) second moment of solute concentration.

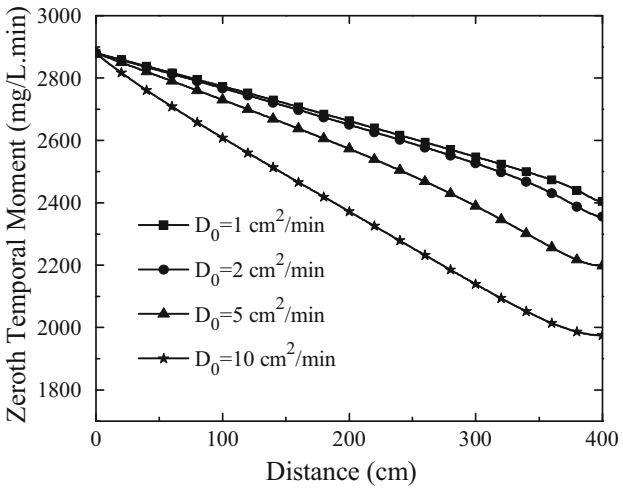
Zeroth Temporal Moment (mg/L.min)
Distance (cm)
D_0=1 cm^2/min
D_0=2 cm^2/min
D_0=5 cm^2/min
D_0=10 cm^2/min

(**a**)

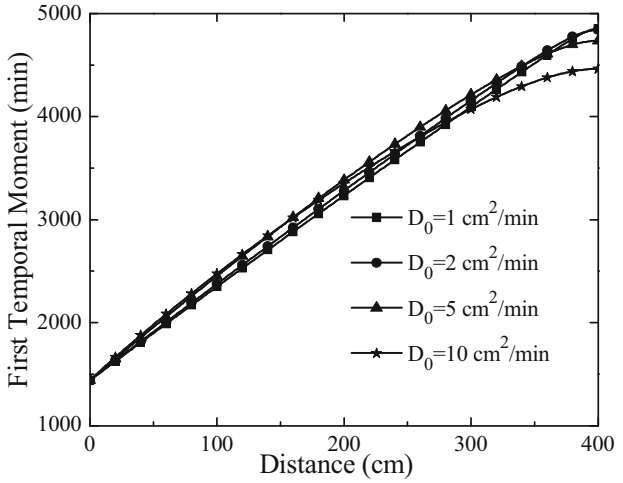
First Temporal Moment (min)
Distance (cm)
D_0=1 cm^2/min
D_0=2 cm^2/min
D_0=5 cm^2/min
D_0=10 cm^2/min

(**b**)

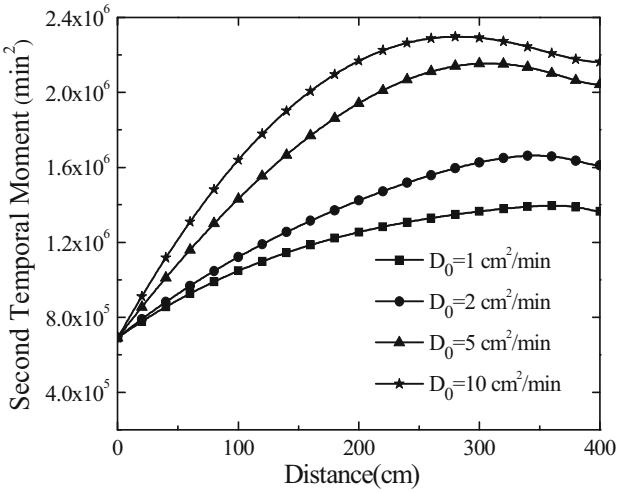
Second Temporal Moment (min^2)
Distance(cm)
D_0=1 cm^2/min
D_0=2 cm^2/min
D_0=5 cm^2/min
D_0=10 cm^2/min

(**c**)

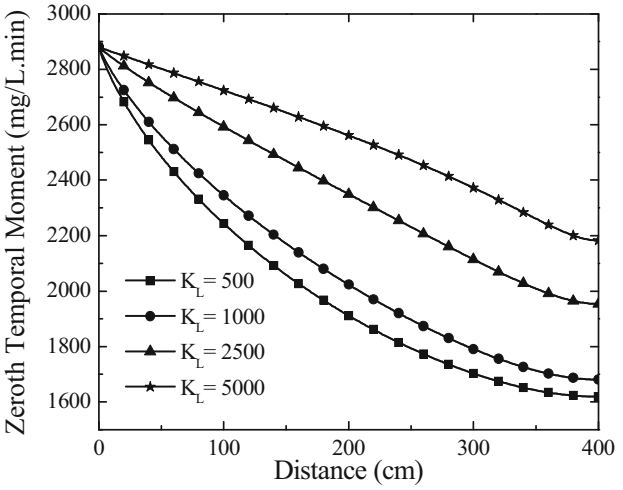
Zeroth Temporal Moment (mg/L.min)
Distance (cm)
K_L= 500
K_L= 1000
K_L= 2500
K_L= 5000

(**d**)

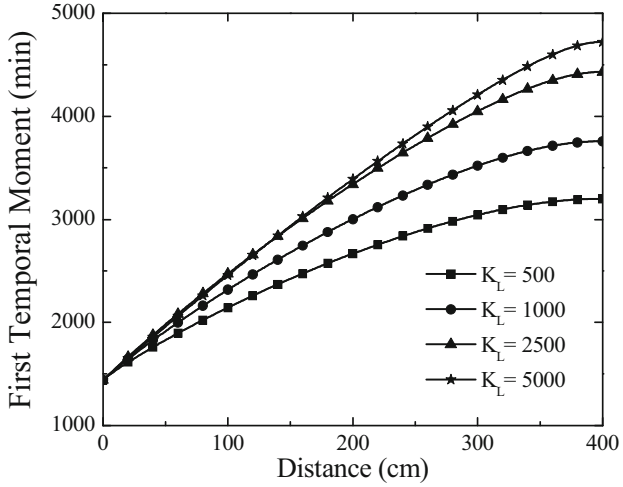
First Temporal Moment (min)
Distance (cm)
K_L= 500
K_L= 1000
K_L= 2500
K_L= 5000

(**e**)

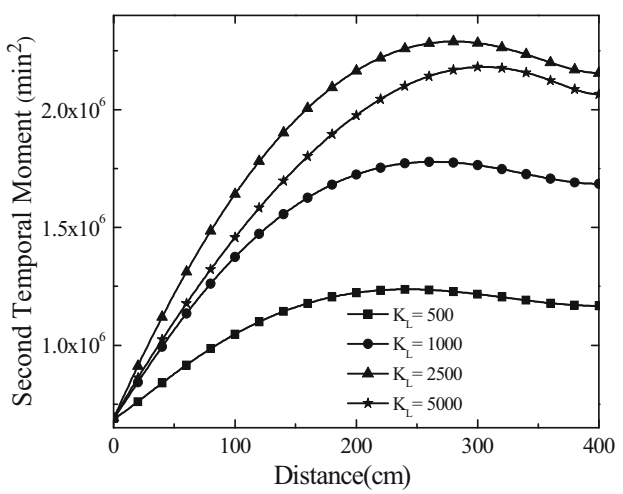
Second Temporal Moment (min^2)
Distance(cm)
K_L= 500
K_L= 1000
K_L= 2500
K_L= 5000

(**f**)

◀**Figure 10.** Effect of time-dependent dispersion coefficients D_0 (a, b, and c) and K_L (d, e, and f) of MIML dispersion model on plume evolution: (**a** and **d**) zeroth moment of solute concentration; (**b** and **e**) first moment of solute concentration; (**c** and **f**) second moment of solute concentration.

effective dispersion is higher for a smaller value of K_A. Therefore, overall dispersion value is higher for K_A= 0 in comparison to K_A= 200. At higher K_A value, magnitude of effective dispersion is less, which cause less spreading of solute. Due to this, more amount of solute mass is advected forward which further leads to less solute mass recovery at particular location with an increase in K_A value. Zeroth temporal moment varies inversely with travel distance as observed from figure 9(d). Spatial variation of first temporal moment for different values of K_A of MIMA model is shown in figure 9(e). First temporal moment is not significantly affected by the time-dependent dispersion coefficient (K_A) of MIMA dispersion model. Figure 9(f) shows the spatial variation of second temporal moment with different values of K_A of MIMA model. The peak value of the second temporal moment is highest for a smaller value of time-dependent dispersion coefficient (K_A). It is observed that the variance of average residence time is consistently lower for the higher value of time-dependent dispersion coefficient (K_A). Non-linear variation of second temporal moment with travel distance is also observed. Slope of the profile increases with travel distance and finally approaches to asymptotic value (at the end of 350 cm as shown in figure 9(f)).

5.2e *Effect of time-dependent dispersion coefficients D_0 and K_L of MIML dispersion model:* Influence of linear time-dependent dispersion parameters (D_0 and K_L) on plume evolution is analyzed using zeroth, first, and second temporal moments. Following input parameters are used in the simulation to study the influence of dispersion coefficient: mass transfer coefficient (ω) = 2.12E-05 min^{-1}, L= 400 cm, K_L =4500, maximum simulation time = 10080 minutes, pulse duration of 2880 minutes, and D_0 value is varied from 1 to 10 cm^2/min.

Figure 10(a) presents the spatial variation of zeroth temporal moment (M_0) for different values of dispersion coefficient (D_0) of MIML model. It is observed that the solute mass recovery decreases with an increase in dispersion coefficient (D_0). It shows that an increase in the value of dispersion coefficient (D_0) of MIML model reduces solute mass in the mobile region. It is also observed that the slope of profile becomes steeper with an increase in dispersion coefficient (D_0) of MIML model. This may be due to linear variation of effective dispersion coefficient without any upper bound limit for MIML model. The value of first temporal moment is highest for smallest value of dispersion coefficient ($D_0 = 1$ cm^2/min) at large travel distances as shown in figure 10(b). It is also observed that the first temporal moment is not significantly affected by dispersion coefficient (D_0) of MIML model. Figure 10(c) shows the spatial distribution of second temporal moment for different values of dispersion coefficient (D_0) of MIML dispersion model. Non-linear variation of second temporal moment with travel distance is observed. The peak of the second temporal moment is highest for a largest value of dispersion coefficient ($D_0 = 10$ cm^2/min). The decrease in second temporal moment at longer travel distances may be due to the removal/ isolation of source from inlet of the porous media system at later travel time. Further, mean travel time (K_L) of MIML model is varied from 500 minutes to 5000 minutes, while keeping other parameters (ω = 2.12E-05 min^{-1}, D_0 = 5.89 cm^2/min) fixed to investigate the impact of K_L on transport behavior.

Figure 10(d) shows the spatial variation of zeroth temporal moment (M_0) with K_L of MIML model. Solute mass recovery varies inversely with travel distance and slope of the profile becomes flatter with increasing K_L value. Significant variation in zeroth temporal moment is observed with change in mean travel time (K_L) of MIML model. Solute mass recovery at particular location increases with an increase in K_L value. This may be due to lower effective dispersion value which cause less spreading/ dilution of the solute plume. Spatial variation of first temporal moment for different values of time-dependent dispersion coefficient (K_L) of MIML model is shown in figure 10(e). It is observed that the average residence time remains the same during very short travel distances (near the inlet solute source), irrespective of the K_L value. It increases with an increase in the value of mean travel time (K_L). It is observed that the slope of the profile becomes steeper with increasing mean travel time (K_L). Figure 10(f) shows the spatial variation of second temporal moment with time-dependent dispersion coefficient (K_L) of MIML dispersion model. Second temporal moment varies non-linearly with travel distance and the slope of the profile decreases as the distance from the source increases and finally approaches to asymptotic value.

6. Conclusions

In this study, temporal moments of solute concentrations are computed numerically to analyze the influence of time-dependent dispersion function on solute plume evolution behavior in heterogeneous porous media. Major findings are summarized as follows.

1. The moment analysis provided a detailed understanding about plume behavior within heterogeneous porous media which BTCs fall short to describe. Effectiveness of MIMA model over MIMC and MIML to simulate transport behavior at field-scale conditions is revealed from temporal moment analysis.
2. Mean arrival time of solute is independent of the time-dependent dispersion coefficient (D_0), as the value of mean arrival time is marginally same for all the

considered solute transport models (i.e., ADEL, ADEA, MIML, and MIMA). However, second temporal moment is dependent upon dispersion function and modelling approach.

3. Computed macro dispersion coefficient is observed as varying non-uniformly with travel distance for all the time-dependent dispersion models which further indicates that the spreading of solute within heterogeneous porous media is scale dependent.
4. It is observed that the first and second temporal moments are less sensitive to asymptotic time-dependent dispersion coefficient (K_A) as compared to other transport parameters such as $K_L, D_0, v_m, \theta_m, \omega$.

Several observations have been made related to solute mass recovery, mean arrival time and spreading of BTC on the basis of numerical simulations. These observations may not be true for other solute transport models involving several complex processes. However, relative impact of the time-dependent dispersion function on transport behavior may be obtained from this study. In future study, effect of specific discharge can be investigated by coupling transient flow equation with solute transport equations.

Acknowledgements

All the work has been carried out at Indian Institute of Technology, Mandi during Master's study of first author. First author would like to thank Indian Institute of Technology, Mandi for supporting this study. The authors would like to thank the reviewer and editor for their constructive and valuable comments.

List of symbols

C_0	Injected concentration of solute source, (M/L^3)
C_m	Solute concentration in the mobile region at any time t, (M/L^3)
C_{im}	Solute concentration in the immobile region at any time t, (M/L^3)
$D_{(t)}$	Time-dependent hydrodynamic dispersion coefficient along the flow velocity, (L^2/T)
D_0	Maximum or uniform dispersion coefficient, (L^2/T)
D_m	Effective diffusion coefficient, (L^2/T)
$D_{macro}(x)$	Macro-dispersion coefficient calculated using second temporal moment
f	Fraction of sorption sites that equilibrate instantly with the mobile regions
K_A	Asymptotic time-dependent dispersion coefficient, (T)
K_{dm}	Distribution coefficient of the linear sorption process in the mobile region, (L^3/M)
K_{dim}	Distribution coefficient of the linear sorption process in the immobile region, (L^3/M)
K_L	Linear time-dependent dispersion coefficient, (T)
M_0	Zeroth absolute temporal moment
M_1	First absolute temporal moment
M_2	Second absolute temporal moment
M_n	nth absolute temporal moment
μ_{lm}	First-order transformation coefficient for solution phase in the mobile region, (T^{-1})
μ_{lim}	First-order transformation coefficient for solution phase in the immobile region, (T^{-1})
μ_{sm}	First-order transformation coefficient for sorbed phase in the mobile region, (T^{-1})
μ_{sim}	First-order transformation coefficient for sorbed phase in the immobile region, (T^{-1})
μ_1	First normalized temporal moment
μ_2	Second normalized temporal moment
μ_n	nth order normalized temporal moment
ω	First order mass transfer coefficient (T^{-1})
q	Flow rate, (L/T)
ρ_b	Bulk density of the porous medium, (M/L^3)
t	Total simulation time, (T)
t_p	Pulse duration, (T)
$T_1(x)$	First temporal moment
$T_2(x)$	Second central temporal moment
θ_m	Volumetric water content of the mobile region
θ_{im}	Volumetric water content of the immobile region
θ	Total volumetric water content of the porous media
v_m	Mobile pore water velocity, (L/T)
$V(x)$	Solute velocity calculated using first temporal moment
x	Spatial coordinate taken in the direction of the fluid flow, (L)

Abbreviations

ADE	Advection dispersion equation
ADEA	Advection-dispersion model with asymptotic time-dependent dispersion
ADEL	Advection-dispersion model with linear time-dependent dispersion
MIM	Mobile–immobile model
MIMA	Mobile–immobile model with asymptotic time-dependent dispersion function
MIMC	Mobile–immobile model with constant dispersion function
MIML	Mobile–immobile model with linear time-dependent dispersion function

References

[1] Kitanidis P K 1994 The concept of the Dilution Index. *Water Resour. Res.* 30:2011–2026. https://doi.org/10.1029/94WR00762

[2] Kapoor V and Gelhar L W 1994 Transport in three-dimensionally heterogeneous aquifers: 1. Dynamics of concentration fluctuations. *Water Resour. Res.* 30:1775–1788. https://doi.org/10.1029/94WR00076

[3] Li Z and Brusseau M L 2000 Nonideal transport of reactive solutes in heterogeneous porous media - 6. Microscopic and macroscopic approaches for incorporating heterogeneous rate-limited mass transfer. *Water Resour. Res.* 36:2853–2867. https://doi.org/10.1029/2000WR900089

[4] Srivastava R and Brusseau M L 1996 Nonideal transport of reactive solutes in heterogeneous porous media: 1. Numerical model development and moments analysis. *J. Contam. Hydrol.* 24:117–143. https://doi.org/10.1016/S0169-7722(96)00039-3

[5] Logan J D 1996 Solute transport in porous media with scale-dependent dispersion and periodic boundary conditions. *J. Hydrol.* 184:261–276. https://doi.org/10.1016/0022-1694(95)02976-1

[6] Ballarini E, Bauer S, Eberhardt C and Beyer C 2014 Evaluation of the Role of Heterogeneities on Transverse Mixing in Bench-Scale Tank Experiments by Numerical Modeling. *Groundwater* 52:368–377. https://doi.org/10.1111/gwat.12066

[7] Bons P D, van Milligen B P and Blum P 2013 A general unified expression for solute and heat dispersion in homogeneous porous media. *Water Resour. Res.* 49:6166–6178. https://doi.org/10.1002/wrcr.20488

[8] Chen J S, Liu C W and Liang C P 2006 Evaluation of longitudinal and transverse dispersivities/distance ratios for tracer test in a radially convergent flow field with scale-dependent dispersion. *Adv. Water Resour.* 29:887–898. https://doi.org/10.1016/j.advwatres.2005.08.001

[9] Sharma P K, Sekhar M, Srivastava R and Ojha C S P 2012 Temporal Moments for Reactive Transport through Fractured Impermeable / Permeable Formations. *J. Hydrol. Eng.* 17:1302–1314. https://doi.org/10.1061/(ASCE)HE.1943-5584.0000586

[10] Pang L, Goltz M and Close M 2003 Application of the method of temporal moments to interpret solute transport with sorption and degradation. *J. Contam. Hydrol.* 60:123–134. https://doi.org/10.1016/S0169-7722(02)00061-X

[11] Valocchi A J 1990 Use of temporal moment analysis to study reactive solute transport in aggregated porous media. *Geoderma* 46:233–247

[12] Yu C, Warrick A W and Conklin M H 1999 A moment method for analyzing breakthrough curves of step inputs. *Water Resour. Res.* 35:3567–3572. https://doi.org/10.1029/1999WR900225

[13] Pang L, Close M and Noonan M 1998 Rhodamine WT and Bacillus subtilis Transport through an Alluvial Gravel Aquifer. *Ground Water* 36:112–122. https://doi.org/10.1111/j.1745-6584.1998.tb01071.x

[14] Renu V and Suresh Kumar G 2016 Temporal Moment Analysis of Multi-Species Radionuclide Transport in a Coupled Fracture-Skin-Matrix System with a Variable Fracture Aperture. *Environ. Model Assess.* 21:547–562. https://doi.org/10.1007/s10666-016-9515-5

[15] Cunningham J A and Roberts P V 1998 Use of temporal moments to investigate the effects of nonuniform grain-size distribution on the transport of sorbing solutes. *Water Resour. Res.* 34:1415–1425

[16] Suresh Kumar G 2014 Mathematical Modeling of Groundwater Flow and Solute Transport in Saturated Fractured Rock Using a Dual-Porosity Approach. *J. Hydrol. Eng.* 19:04014033. https://doi.org/10.1061/(ASCE)HE.1943-5584.0000986

[17] Govindaraju R S, Das B S 2007 *Moment Analysis For Subsurface Hydrologic Applications*. Springer Netherlands, Dordrecht

[18] Naff R L 1992 Arrival times and temporal moments of breakthrough curves for an imperfectly stratified aquifer. *Water Resour. Res.* 28:53–68. https://doi.org/10.1029/91WR02105

[19] Valocchi A J 1985 Validity of the Local Equilibrium Assumption for Modeling Sorbing Solute Transport Through Homogeneous Soils. *Water Resour. Res.* 21:808–820. https://doi.org/10.1029/WR021i006p00808

[20] Joshi N, Ojha C S P, Sharma P K and Madramootoo C A 2015 Application of nonequilibrium fracture matrix model in simulating reactive contaminant transport through fractured porous media. *Water Resour. Res.* 51:390–408. https://doi.org/10.1002/2014WR016500/abstract

[21] Renu V and Kumar G S 2014 Temporal moment analysis of solute transport in a coupled fracture-skin-matrix system. *Sadhana* 39:487–509. https://doi.org/10.1007/s12046-014-0240-y

[22] Sharma P K, Ojha C S P and Joshi N 2014 Finite volume model for reactive transport in fractured porous media with distance- and time-dependent dispersion. *Hydrol. Sci.* J. 59:1582–1592. https://doi.org/10.1080/02626667.2014.932910

[23] Kumar G S, Sekhar M and Misra D 2006 Time dependent dispersivity behavior of non-reactive solutes in a system of parallel fractures. *Hydrol. Earth Syst. Sci. Discuss.* 3:895–923. https://doi.org/10.5194/hessd-3-895-2006

[24] Jaiswal D K, Kumar A, Kumar N and Yadav R R 2009 Analytical solutions for temporally and spatially dependent solute dispersion of pulse type input concentration in one-dimensional semi-infinite media. *J. Hydro-Environment Res.* 2:254–263. https://doi.org/10.1016/j.jher.2009.01.003

[25] Barry D A and Sposito G 1989 Analytical Solution of a Convection-Dispersion Model With Time-Dependent Transport Coefficients. *Water Resour Res.* 25:2407–2416

[26] Natarajan N 2016 Effect of distance-dependent and time-dependent dispersion on non-linearly sorbed multispecies contaminants in porous media. *ISH J. Hydraul. Eng.* 22:16–29. https://doi.org/10.1080/09715010.2015.1043597

[27] Basha H A and El-Habel F S 1993 Analytical solution of the one-dimensional time-dependent transport equation. *Water Resour. Res.* 29:3209–3214. https://doi.org/10.1029/93WR01038

[28] van Genuchten M T and Wierenga P J 1976 Mass Transfer Studies in Sorbing Porous Media I. Analytical Solutions. *Soil Sci. Soc. Am. J.* 40:473–480. https://doi.org/10.2136/sssaj1976.03615995004000040011x

[29] van Genuchten M T and Wierenga P J 1977 Mass Transfer Studies in Sorbing Porous Media: II. Experimental Evaluation with Tritium. *Soil Sci. Soc. Am. J.* 41:272–278

[30] Guleria A, Swami D, Sharma A and Sharma S 2019 Non-reactive solute transport modelling with time-dependent

dispersion through stratified porous media. *Sādhanā* 44:81. https://doi.org/10.1007/s12046-019-1056-6

[31] Zheng C and Bennett G D 2002 *Applied Contaminant Transport Modeling*, 2nd ed. Wiley-Interscience, New York

[32] Swami D, Sharma P K and Ojha C S P 2016 Behavioral Study of the Mass Transfer Coefficient of Nonreactive Solute with Velocity, Distance, and Dispersion. *J. Environ. Eng.* 143:1–10. https://doi.org/10.1061/(ASCE)EE.1943-7870.0001164